available at www.sciencedirect.com

ScienceDirect

www.elsevier.com/locate/brainres

BRAIN RESEARCH

Research Report

Synaptic contribution of Ca^{2+}-permeable and Ca^{2+}-impermeable AMPA receptors on isolated carp retinal horizontal cells and their modulation by Zn^{2+}

*Yan Sun, Xiao-Dong Jiang, Xue Liu, Hai-Qing Gong, Pei-Ji Liang**

School of Life Sciences and Biotechnology, Shanghai Jiao Tong University, 800 Dong-Chuan Road, Shanghai 200240, China

ARTICLE INFO

Article history:
Accepted 21 December 2009
Available online 4 January 2010

Keywords:
Glutamate current
Patch-clamp recording
1-naphthyl acetyl spermine
Pentobarbital

ABSTRACT

Ca^{2+}-permeable and Ca^{2+}-impermeable AMPA receptors are co-expressed on carp retinal horizontal cells. In the present study, we examined the synaptic contribution and Zn^{2+} modulatory effect of these two AMPA receptor subtypes using whole-cell patch clamp technique. Specific Ca^{2+}-permeable AMPA receptor antagonist (1-naphthyl acetyl spermine, NAS) and selective Ca^{2+}-impermeable AMPA receptor blocker (pentobarbital, PB) were used to separate the glutamate-response in isolated H1 horizontal cell mediated by these two subtypes of AMPA receptors respectively. Application of 100 μM NAS substantially suppressed the current elicited by 3 mM glutamate and the remaining NAS-insensitive component was completely blocked by application of 100 μM PB. In addition, Zn^{2+} had dual effects on Ca^{2+}-permeable AMPA receptor-mediated current: at low concentration (10 μM), Zn^{2+} potentiated the current, but at higher concentrations (100 and 1000 μM), Zn^{2+} reduced the current in a dose-dependent manner. However, Zn^{2+} (10, 100 and 1000 μM) failed to modulate the NAS-insensitive current mediated by Ca^{2+}-impermeable AMPA receptors. Overall, our results suggest that Ca^{2+}-permeable AMPA receptors contribute more to the cell's glutamate-response than Ca^{2+}-impermeable AMPA receptors. Furthermore, Zn^{2+} has dual effects on the Ca^{2+}-permeable AMPA receptor activity without affecting Ca^{2+}-impermeable AMPA receptors.

1. Introduction

AMPA receptors (AMPARs) mediate the majority of fast excitatory neurotransmission at glutamatergic synapses in the central nervous system (CNS). AMPAR, as a tetramer, can be homo- or hetero-assembled by four types of subunits (termed GluR1–4). It displays low Ca^{2+} permeability in the presence of GluR2 subunit and is with high Ca^{2+} permeability in the absence of GluR2. That is because RNA editing at the Q/R site of GluR2 subunit (a glutamine (Q) replaced by an arginine (R) at the Q/R site) makes the characteristics of AMPARs different (Hollmann and Heinemann, 1994; Geiger et al., 1995).

Horizontal cells (HCs) are the second-order neurons in the inner nuclear layer of vertebrate retinas and respond to glutamate released from photoreceptors with membrane depolarization in the dark. Their activities regulate the visual signals laterally and determine the antagonistic receptive field structure of bipolar and ganglion cells. Furthermore, it is well accepted that the non-NMDA glutamate receptors

* *Corresponding author*. Fax: +86 21 34204016.
E-mail address: pjliang@sjtu.edu.cn (P.-J. Liang).

0006-8993/$ – see front matter © 2009 Elsevier B.V. All rights reserved.
doi:10.1016/j.brainres.2009.12.068

expressed on carp retinal HCs are AMPA-preferring subtype (Lu et al., 1998).

Previous work of our laboratory, using Fura-2 fluorescent Ca^{2+} imaging technique, revealed that Ca^{2+}-permeable AMPARs and Ca^{2+}-impermeable AMPARs (CP- and CIP-AMPARs) co-existed in carp retinal HCs (Huang and Liang, 2005). However, the respective contribution of CP- and CIP-AMPARs to the HC's glutamate-response still needs investigation.

In vertebrate retinas, Zn^{2+} is co-localized with glutamate vesicles in photoreceptor terminals and also proved to be released from there, which suggests that Zn^{2+} may play modulatory roles in the outer retina (Wu et al., 1993; Redenti et al., 2007; Lee et al., 2008). The effects that Zn^{2+} exerts on glutamate receptors in vertebrate HCs are diversified. In retinal HCs of hybrid striped bass, Zn^{2+} at micro-molar concentrations partially suppressed the AMPAR-mediated responses and also reduced the AMPAR's affinity to glutamate (Zhang et al., 2002). But in perch retinal HCs, Zn^{2+} was ineffective in modulating the activity of glutamate receptors, even at a concentration of 1 mM (Schmidt, 1999).

In addition, it was reported that in carp retinal HCs, Zn^{2+} effect was associated with the flip/flop variants of AMPARs, with the latter being resulted from alternative splicing mRNA and exhibiting different dynamic and pharmacological properties (Sommer et al., 1990; Partin et al., 1995; Shen and Yang, 1999; Dingledine et al., 1999). Apart from the structure-dependent (splicing variants) effect, it is also important to know whether Zn^{2+} modulatory effects are related to the functional variations of AMPARs (CP-/CIP-AMPARs).

In the present study, we first examined the contributions of the CP- and CIP-AMPARs in mediating glutamate-response on carp retinal H1 horizontal cells (H1 cells) and then investigated the modulatory effects that Zn^{2+} exerts on different subtypes of AMPARs. Application of 1-naphthyl acetyl spermine (NAS), a specific CP-AMPAR blocker and pentobarbital (PB, at a concentration of 100 μM), a selective CIP-AMPAR antagonist could both partially inhibit H1 cells' response elicited by 3 mM glutamate. The suppression effects demonstrate that CP-AMPARs mediate the majority of the total glutamate current, which suggests the importance of CP-AMPARs in signal transmission on retinal HCs. Furthermore, Zn^{2+} has dual effects on the CP-AMPAR-mediated current, but has no observable effect on the CIP-AMPAR-mediated component. It implies that Zn^{2+} is involved in different but important modulations of the glutamate-response through CP-AMPAR in carp retinal H1 cells: zinc potentiation of CP-AMPARs may regulate the synaptic plasticity of HCs, whereas zinc inhibition of these receptors might protect the neurons from cell death under excitotoxicity-induced neurodegeneration.

2. Results

2.1. Contributions of the CP- and CIP-AMPARs to glutamate-response in H1 cells

Previous work of our laboratory, using Ca^{2+} imaging technique, has revealed that CP- and CIP-AMPARs are co-expressed on carp retinal H1 cells (Huang and Liang, 2005). In the present study, we further examined the synaptic contribution of CP- and CIP-AMPARs to mediate the glutamate-current in isolated H1 cells using whole-cell recording technique.

2.1.1. CP-AMPARs mediated the majority of the glutamatergic response

In order to evaluate the CP-AMPAR-mediated current in H1 cells, CP-AMPAR blocker NAS, a synthetic analogue of joro spider toxin (Koike et al., 1997), was applied in our experiments. The blockade effect that NAS exerts on CP-AMPAR was concentration-dependent and this inhibitory effect is presented in Fig. 1 and Table 1. The averaged data (peak currents elicited by 3 mM glutamate) were well fitted by the curve $R = \frac{100\% - R_{min}}{1 + (NAS/IC_{50})^n} + R_{min}$, with R_{min} being 25.0%, IC_{50} being 1.45 μM, and n being 0.92. The results show that NAS at a concentration of 100 μM completely blocked the H1 cells' CP-AMPAR response elicited by 3 mM glutamate (Fig. 1, gray trace) and thus 100 μM NAS was applied in the subsequent experiments.

A typical experimental recording is plotted in Fig. 2A. Application of 3 mM glutamate elicited an inward current in an isolated H1 cell with peak current being 405.9 pA. When 100 μM NAS was pre-superfused for 1 min, the application of 3 mM glutamate elicited a peak current of only 99.8 pA. The remaining NAS-insensitive current was then completely suppressed by additional application of 100 μM PB (1 min prior to and during the glutamate application). After NAS and PB were washed out by the Ringer's solution for more than 1 min, the peak current elicited by 3 mM glutamate was partially recovered to 262.7 pA. Statistical data presented in Fig. 2C (white columns) show that the glutamate-elicited peak current was reduced to 25.0±10.5% of the control level during NAS application ($p<0.05$, $n=5$), whereas the peak current was completely eliminated in the presence of NAS + PB, and recovered to 66.2±11.5% of the control level after NAS + PB was washed out for more than 1 min. This result suggests that the CP-AMPARs contributed a large portion (75.0±10.5%) to the glutamatergic current in the isolated H1 cells.

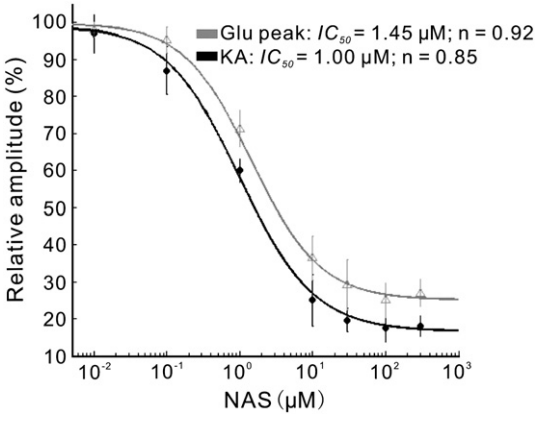

Fig. 1 – The dose-dependent inhibitory effect of NAS on glutamate-current. The responses were elicited by 3 mM Glu (peak current value, gray line) and 100 μM KA (black line). The averaged data (mean±SE, n=5 for each) were well fitted by the curve described by $R = \frac{100\% - R_{min}}{1 + (NAS/IC_{50})^n} + R_{min}$.

Table 1 – NAS dose-dependently inhibits the currents elicited by glutamate/KA.

Agonists	NAS (μM)				
	0.01	0.1	1	10	30
Glu	98.1±5.7%	90.2±9.9%	71.3±14.2%	36.4±13.2%	29.2±15.2%
KA	97.1±11.6%	87.2±14.3%	60.5±7.0%	25.0±15.6%	19.6±7.1%
Agonists	NAS (μM)		R_{min}	IC_{50}	n
	100	300			
Glu	25.0±10.5%	26.9±8.3%	25.0%	1.45 μM	0.92
KA	17.6±11.0%	18.0±6.2%	17.6%	1.00 μM	0.85

Note. "Glu" represents the data from glutamate (3 mM) elicited currents; "KA" represents the data from KA (100 μM) elicited currents (n = 5 for each data, mean ± SD).

2.1.2. *The CIP-AMPARs mediated the minority of the glutamatergic current*

From the results given in Fig. 2A and C, it is clearly shown that the NAS-insensitive glutamate-current mediated by CIP-AMPARs contributed a small proportion to the whole glutamate-response. Pentobarbital (PB), which selectively suppresses CIP-AMPAR at a concentration of 100 μM (Taverna et al., 1994; Yamakura et al., 1995; Van Damme et al., 2002), was also applied to directly examine the synaptic contribution of CIP-AMPARs to the cell's glutamate-response. An example is given in Fig. 3A. During control, the application of 3 mM glutamate elicited an inward current in an H1 cell with peak value of 515.6 pA. After 10 s pre-superfusion of 100 μM PB, the peak current was reduced to 380.1 pA and was almost completely recovered when PB was washed out for 15 s (peak current 494.3 pA). The statistical results given in Fig. 3C (white columns) show that the peak value of the glutamate-response was reduced to 73.2±3.1% ($p<0.05$) after the application of 100 μM PB and recovered to 91.7±8.1% of the control level after 15 s Ringer's wash-out ($n=5$). This confirms that the CIP-AMPARs expressed on H1 cells mediated the minority (26.8±3.1%) of the glutamatergic response.

2.1.3. *The suppression effect of NAS and PB on KA-elicited current*

It is well known that kainate (KA), a full agonist of AMPAR, can elicit the maximal AMPA-current without desensitization (Hollmann and Heinemann, 1994). Therefore, 100 μM KA was also applied to avoid the potential underestimation of the peak value of AMPA-current.

The NAS effect on KA-elicited current was also tested (see Fig. 1 and Table 1). The results show that 100 μM NAS could completely block the H1 cells' CP-AMPAR response elicited by 100 μM KA (Fig. 1, black trace) and thus 100 μM NAS was applied in the subsequent experiments. As shown in Fig. 2B, application of 100 μM KA elicited a non-desensitizing current of 599.8 pA in an isolated H1 cell and the current was reduced to 109.1 pA after pre-superfusion of 100 μM NAS for 1 min. When 100 μM NAS + 100 μM PB were co-applied for 1 min prior to and during KA application, the current was completely inhibited. After NAS and PB were washed out for more than 1 min, the KA-elicited current was partially recovered to 410.0 pA. Statistical data presented in Fig. 2C (gray columns) show that the KA-elicited current was reduced to 17.6±11.0% ($p<0.05$, $n=8$) of the control level during NAS application, which was then completely inhibited by co-application of NAS + PB and partially recovered

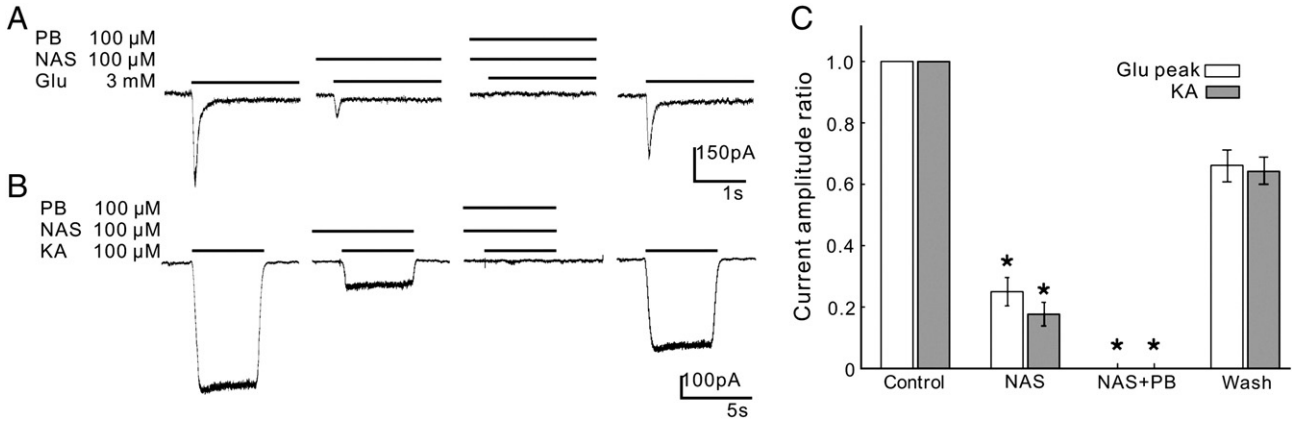

Fig. 2 – Glutamate-response mediated by CP-AMPARs. (A) An example of the Glu-currents measured during control, in the presence of NAS, NAS + PB and after washout. (B) KA-elicited currents measured under the same protocol as in (A). (C) Normalized data of NAS suppression (mean ± SE) of the Glu-current (peak current, $n=5$, white columns) and KA-elicited current ($n=8$, gray columns) ($^*p<0.05$, paired t-test, as compared to control).

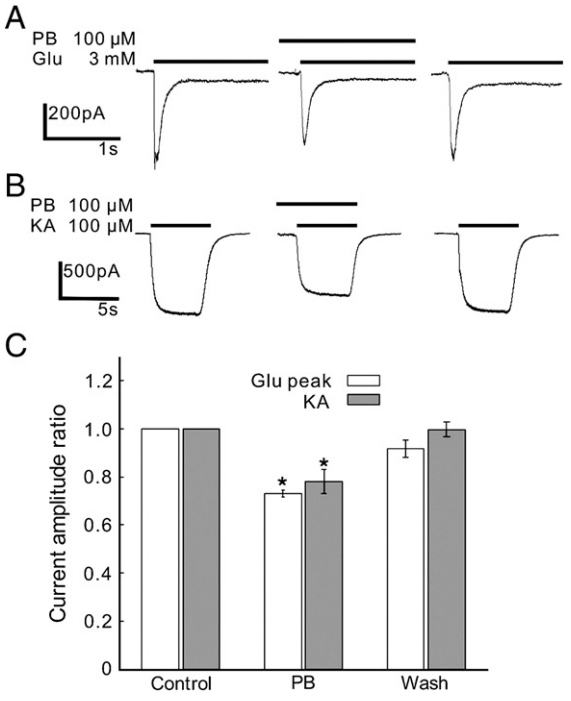

Fig. 3 – Glutamate-response mediated by CIP-AMPARs. (A) Glu-currents measured during control, in the presence of PB and after washout. (B) KA-elicited currents measured under the same protocol as in (A). (C) Normalized data of PB inhibition of the Glu-current (peak current, $n=5$, white column) and KA-elicited current ($n=8$, gray column) (*$p<0.05$, paired t-test, as compared to control).

to 64.4±12.4% of the control level after Ringer's wash-out for more than 1 min. These results confirm the point that CP-AMPARs contributed the majority (82.4±11.0%) to the KA-elicited current in the isolated H1 cells, which is compatible to the results of glutamate-elicited currents (see Fig. 2A).

In Fig. 3B, the PB effect exerted on the KA-elicited current was also detected. Application of 100 μM KA induced a current of 1014.3 pA in an H1 cell, which was attenuated to 750.0 pA after pre-superfusion of 100 μM PB for 10 s and the reduced current was almost completely recovered (994.3 pA) after washing out for 15 s. The statistical data given in Fig. 3C (gray columns) show that the KA-elicited current was reduced to 77.9±14.2% ($p<0.05$) after PB inhibition and recovered to 99.8±8.5% of the control level after 15 s Ringer's wash-out ($n=8$). These results also reflect that the CIP-AMPAR-mediated response contributes a small portion (22.1±14.2%) to the whole KA-elicited response, which is compatible to the results of the glutamate-elicited current (see Fig. 3A).

All these results demonstrated that the CP-AMPARs contribute more to cell's glutamate-response than the CIP-AMPARs do.

2.2. Zn^{2+} modulatory effect on the CP- and CIP-AMPAR-mediated currents

Zn^{2+}, as an endogenous neuromodulator in the retina, has diversified modulatory effects on various ion channels and its modulatory effects are also related to the splice-variants of AMPARs on retinal HCs (Shen and Yang, 1999; Ugarte and Osborne, 2001; Grahn et al., 2001). In our experiments, we tried to test if the modulatory effects that Zn^{2+} exerts on AMPARs are dependent on the functional variants of these receptors.

2.2.1. Zn^{2+} had dual effects on the current mediated by CP-AMPARs

To isolate the glutamate-response mediated by CP-AMPARs, 100 μM PB was used to block the CIP-AMPAR-mediated response. As shown in Fig. 4A(a), in the presence of 100 μM PB, application of 3 mM glutamate elicited a peak current of 326.5 pA. After pre-superfusion of 10 μM Zn^{2+} for 10 s, the peak current was almost kept unaltered (307.7 pA) but the desensitization of the current was diminished and such change was mostly recovered after Zn^{2+} was washed away for more than 1 min (peak current 308.1 pA). Statistical data given in Fig. 4C (white columns) show that the application of 10 μM Zn^{2+} has no significant effect on the peak value of the CP-AMPAR-mediated current (99.5±11.2% of the control level, $p>0.05$, $n=5$), however, the desensitization was completely eliminated. The peak current was recovered to 97.1±5.2% of the control level after washing out Zn^{2+} for more than 1 min ($p>0.05$, $n=5$).

Further experiments were performed on H1 cells with application of Zn^{2+} at concentrations of 100 μM and 1 mM, and the representative results are shown in Fig. 4A(b–c). In the presence of 100 μM PB, application of 3 mM glutamate elicited a peak current of 444.4 pA and after pre-superfusion of 100 μM Zn^{2+} for 10 s, co-application of 3 mM glutamate elicited a peak current of 315.6 pA. The peak current was recovered to 356.8 pA after Zn^{2+} was washed away for more than 1 min (see Fig. 4A(b)). Statistical data given in Fig. 4C (white columns) show that the application of 100 μM Zn^{2+} reduced the peak value of the CP-AMPAR-mediated current to 72.2±4.7% ($p<0.05$, $n=5$) of the control level. The recovery rate of the peak current was 90.0±9.8% of the control level after Zn^{2+} was washed out for more than 1 min ($p>0.05$, $n=5$).

When Zn^{2+} concentration was increased to 1 mM, its inhibitory effect was also increased. Application of 3 mM glutamate elicited a peak current of 265.4 pA in the presence of 100 μM PB and the peak current was then reduced to 69.2 pA after pre-superfusion of 1 mM Zn^{2+} for 10 s (Fig. 4A(c)). The peak current elicited by 3 mM glutamate was recovered to 253.8 pA after Zn^{2+} was washed away for more than 1 min. Statistical data given in Fig. 4C (white columns) show that 1 mM Zn^{2+} effectively inhibited the CP-AMPAR-mediated response to 21.1±9.7% of the control level ($p<0.05$, $n=5$). The peak current was recovered to 97.9±6.4% of the control level after washing out for more than 1 min ($p>0.05$, $n=5$).

2.2.2. Zn^{2+} did not affect the NAS-insensitive current mediated by CIP-AMPARs

To investigate whether Zn^{2+} affects the CIP-AMPAR-mediated current, the response mediated by CP-AMPARs was suppressed by 100 μM NAS. A representative result is shown in Fig. 5A(a). The peak value of the control current elicited by 3 mM glutamate in the presence of 100 μM NAS was 200.0 pA and the peak current was almost kept unchanged (192.7 pA) during application of 10 μM Zn^{2+} (10 s prior to and during the glutamate application). After Zn^{2+} was washed away for more than 1 min, the peak value of the CIP-AMPAR-mediated

current was measured as 198.4 pA. The statistical results in Fig. 5C (white columns) show that the peak value of the CIP-AMPAR-mediated current during the application of 10 μM Zn^{2+} was not significantly changed (96.5±6.3%, $p>0.05$, $n=5$) as compared to the control. The recovery rate of peak current was 98.3±2.1% of the control level after washing out for more than 1 min ($p>0.05$, $n=5$).

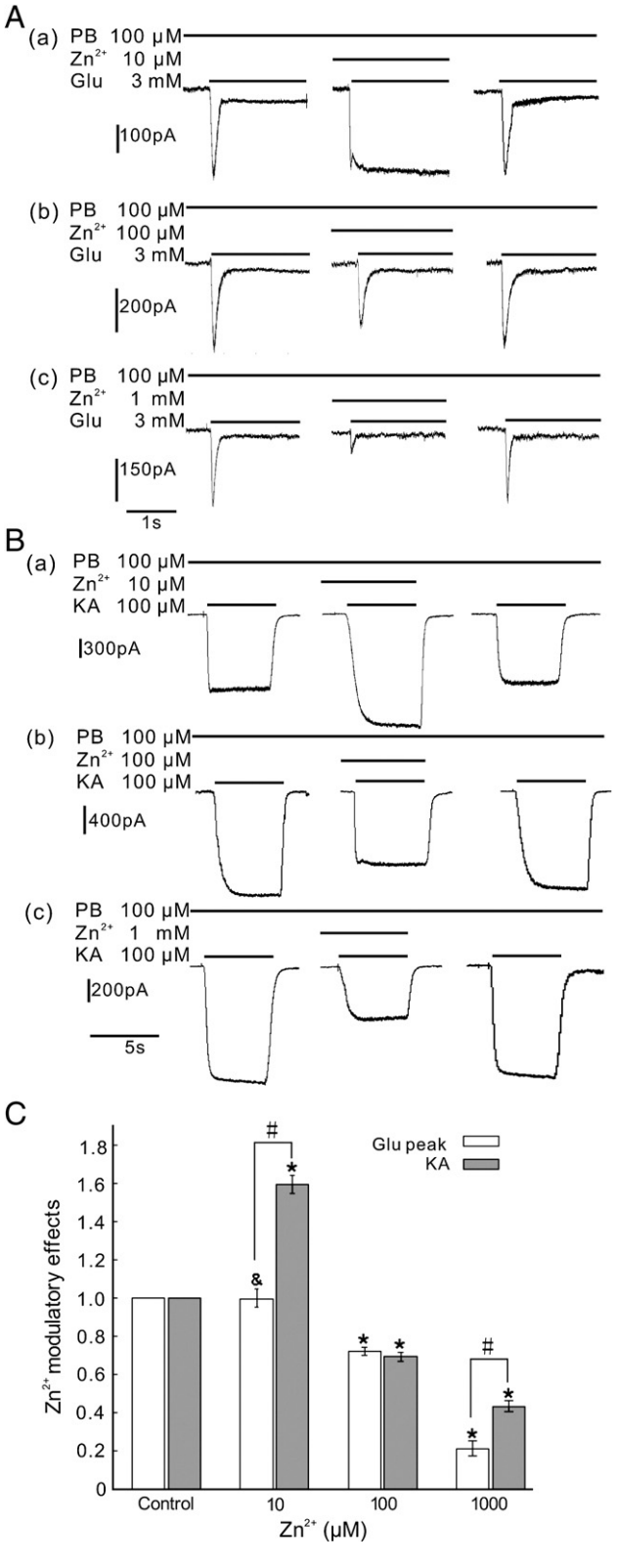

Furthermore, Zn^{2+} effect was also tested at a concentration of 1 mM. In the presence of 100 μM NAS, glutamate (3 mM) elicited an inward current with peak value of 130.9 pA, which was almost unchanged after pre-superfusion of 1 mM Zn^{2+} for 10 s (peak value of 128.6 pA). When Zn^{2+} was washed away for more than 1 min, the peak value of the CIP-AMPAR-mediated current was measured as 129.5 pA (see Fig. 5A(b)). The statistical results given in Fig. 5C (white columns) show that the peak value of the CIP-AMPAR-mediated current was 97.1±4.8% ($p>0.05$, $n=5$) of the control level during the application of 1 mM Zn^{2+}. The recovery rate was 98.9±1.8% of the control level after washing out for more than 1 min ($p>0.05$, $n=5$).

These results suggest that Zn^{2+} has no significant modulatory effect on the CIP-AMPAR-mediated current.

2.2.3. *Zn^{2+} effects on KA-elicited current mediated by CP- and CIP-AMPARs*

Zn^{2+} effects on KA-elicited current were also examined, to avoid the potential underestimation of the peak value of glutamate-elicited AMPA-current.

The Zn^{2+} effects exerted on KA-elicited current mediated by CP-AMPARs are plotted in Fig. 4B(a–c). In the presence of 100 μM PB, KA (100 μM) elicited an inward current of 1200.9 pA, which was enhanced to 1790.4 pA after pre-application of 10 μM Zn^{2+} for 10 s and recovered to 1050.7 pA after more than 1 min Ringer's wash-out (Fig. 4B(a)). The statistical results given in Fig. 4C (gray columns) show that the KA-elicited current mediated by CP-AMPARs was potentiated to 159.7±13.9% ($p<0.05$, $n=8$) of the control level in the presence of 10 μM Zn^{2+}, such potentiation was more significant than the Zn^{2+} effect exerted on the CP-AMPAR-response elicited by glutamate ($p<0.05$, unpaired *t*-test, indicated by "#" in Fig 4C). The recovery rate of KA-elicited current was 90.7±6.4% of the control level after Zn^{2+} had been washed out for more than 1 min ($p>0.05$, $n=8$).

At higher concentrations (100 μM and 1 mM), Zn^{2+} also showed inhibitory effects on the CP-AMPAR-mediated current elicited by 100 μM KA as shown in Fig. 4B(b–c). In an example cell, KA-elicited currents in the presence of 100 μM PB were measured as 1420.0, 980.0 and 1320.0 pA during control, after 10 s application of 100 μM Zn^{2+}, and after 1 min wash-out, respectively (Fig. 4B(b)). While in another cell, the KA-elicited currents in the presence of 100 μM PB were recorded as 1066.7, 500.0 and 1033.3 pA during control, after 10 s application of 1 mM Zn^{2+}, and after 1 min wash-out,

Fig. 4 – Zn^{2+} effects on CP-AMPAR-mediated responses. (A, a–c): In the presence of PB, Glu-current was potentiated by 10 μM Zn^{2+} with desensitization process eliminated. At a higher concentration (100 μM), Zn^{2+} turned to inhibit the CP-AMPAR-mediated responses and the inhibitory effect was more profound in the presence of 1 mM Zn^{2+}. (B, a–c): KA-elicited responses also show the dual effects of Zn^{2+} modulation. (C) Normalized Zn^{2+} effects on Glu-current (peak current, $n=5$, white column) and KA-elicited current ($n=8$, gray column) ($^{*}p<0.05$, $^{\&}p>0.05$, paired *t*-test, as compared to control). $^{\#}p<0.05$ (unpaired *t*-test, comparison between data as indicated).

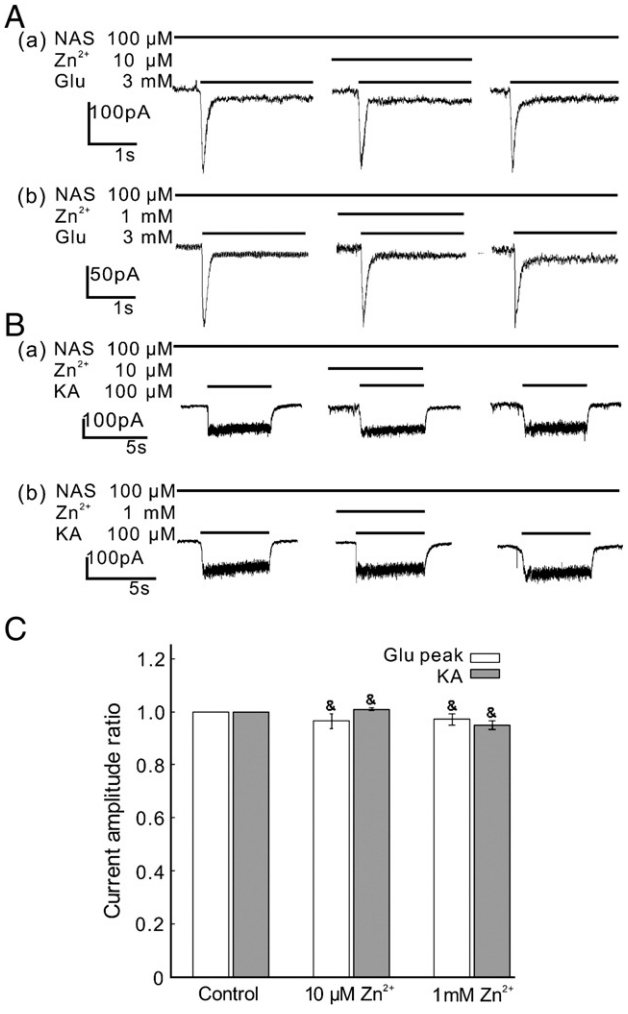

Fig. 5 – Zn^{2+} had no modulatory effect on CIP-AMPAR activity. (A, a–b): In the presence of NAS, Glu-currents from two H1 cells were kept unchanged after application of 10 μM Zn^{2+} as well as 1 mM Zn^{2+}. (B, a–b): KA-elicited current was not changed by Zn^{2+} (10 μM and 1 mM). (C) Normalized data of Zn^{2+} modulatory effect on CIP-AMPAR-mediated responses elicited by Glu (peak current, $n=5$, white column) and KA ($n=8$, gray column) ($^{\&}p>0.05$, paired t-test, as compared to control).

respectively (Fig. 4B(c)). The statistical results given in Fig. 4C (gray columns) show that the application of 100 μM and 1 mM Zn^{2+} suppressed the CP-AMPAR-mediated currents (KA-elicited) to 69.2±7.0% and 43.2±7.8% of the control level respectively ($p<0.05$, $n=8$ for each). The recovery rates of CP-AMPAR-mediated current (KA-elicited) were 93.0±14.3% (100 μM Zn^{2+}) and 91.3±7.3% (1 mM Zn^{2+}) of the control level after Zn^{2+} had been washed out for more than 1 min ($p>0.05$, $n=8$ for each). The inhibitory effect that 1 mM Zn^{2+} exerted on CP-AMPAR-response elicited by KA was less significant than that elicited by glutamate ($p<0.05$, unpaired t-test, indicated by "#" in Fig 4C).

KA (100 μM) was also applied to confirm the Zn^{2+} effect on CIP-AMPAR-mediated current in the presence of 100 μM NAS. Representative results are shown in Fig. 5(B). In an example cell, the CIP-AMPAR-mediated currents elicited by 100 μM KA were measured as 122.4, 125.7 and 120.1 pA during control, after 10 s application of 10 μM Zn^{2+}, and after 1 min wash-out, respectively (Fig. 5B(a)). While in another cell, the CIP-AMPAR-mediated currents elicited by 100 μM KA were tested as 125.9, 122.7 and 120.0 pA during control, after 10 s application of 1 mM Zn^{2+}, and after 1 min wash-out, respectively (Fig. 5B(b)). The statistical results given in Fig. 5C (gray columns) show that Zn^{2+} has no significant modulatory effect on CIP-AMPAR-response at either 10 μM or 1 mM (101.1±1.5% and 95.1±5.0% of the control level, respectively, $p>0.05$, $n=8$ for each). The recovery rates of KA-elicited current in the presence of 100 μM NAS were 98.8±1.9% (10 μM Zn^{2+}) and 95.3±4.8% (1 mM Zn^{2+}) of the control level after Ringer's wash-out for more than 1 min ($p>0.05$, $n=8$ for each).

All the above results suggest that Zn^{2+} has dual effects on the glutamatergic response mediated by the CP-AMPARs without affecting that mediated by the CIP-AMPARs in isolated carp retinal HCs.

2.2.4. *Zn^{2+} did not affect the CP-AMPAR's affinity for glutamate*

In the present study, Zn^{2+} at low (10 μM) and high (≥100 μM) concentrations exerted dual effects on CP-AMPARs of carp retinal H1 HCs. To explore whether Zn^{2+} modulates the CP-AMPAR's affinity for glutamate, we examined the dose-dependence of the glutamate response (with 100 μM PB) in the absence and presence of 500 μM Zn^{2+} (see Fig. 6 and Table 2). The averaged data (peak currents elicited by glutamate) were well fitted by the curve $I=I_{max}/[1+(EC_{50}/Glu)^n]$. In the presence of 500 μM Zn^{2+}, the receptor's affinity for glutamate was not changed as compared to the control level, with the EC_{50} being 700.0 μM in both the conditions. Meanwhile, the n value was little bit changed from 1.40 in the control to 1.35 in the presence of 500 μM Zn^{2+}. However, in the presence of 500 μM Zn^{2+}, the maximal peak current (I_{max}) elicited by 20 mM glutamate was significantly reduced to 49.0±8.5% of the control level (from 510.0±56.3 pA to 250.0±28.1 pA, mean

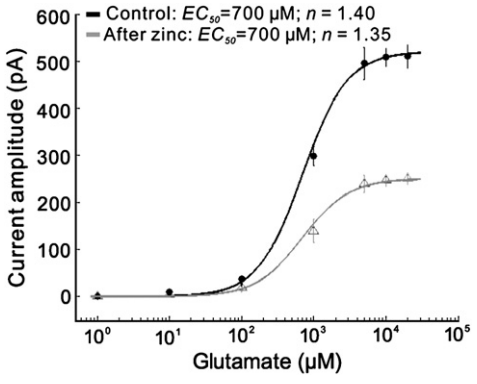

Fig. 6 – Zn^{2+} (500 μM) reduced the maximal peak current mediated by CP-AMPARs on H1 cells without changing the receptor's affinity for glutamate. Dose–response curves for glutamate in the absence (black curve) and presence (gray curve) of 500 μM Zn^{2+}. The averaged data (mean±SE, $n=5$ for each) were fitted by the curve described by $I=\frac{I_{max}}{1+(EC_{50}/Glu)^n}$.

Table 2 – Dose-dependence of glutamate-responses mediated by CP-AMPARs.

	Glu (μM)				
	1	10	100	1000	5000
Glu (pA)	0	10.0±8.5	36.9±13.7	297.8±45.8	495.2±77.4
Glu + Zn^{2+}(pA)	0	5.0±2.2	20.0±10.1	140.0±55.9	238.6±42.0

	Glu (μM)		I_{max}	EC_{50}	n
	10000	20000			
Glu (pA)	507.9±44.7	510.0±56.3	510.0	700.0 μM	1.40
Glu + Zn^{2+}(pA)	246.6±28.0	250.0±28.1	250.0	700.0 μM	1.35

Note. "Glu" represents the glutamate-currents in the control condition; "Glu + Zn^{2+}" represents the glutamate-currents under 500 μM Zn^{2+} (n=5 for each data, mean±SD).

±SD, $p<0.05$, paired t-test). On the other hand, during application of 10 μM Zn^{2+}, which potentiates the CP-AMPAR-responses by eliminating the receptor's desensitization, both the glutamate affinity and the maximal peak current showed no change as compared to the control level (data was not shown). Overall, the dual effects that Zn^{2+} exerted on CP-AMPARs did not change the receptor's affinity for glutamate on carp retinal H1 HCs.

3. Discussion

The main results of the present study are: (1) in isolated carp retinal H1 cells, the CP-AMPARs contribute more to the cell's glutamate-response than the CIP-AMPARs do; (2) Zn^{2+} exerts dual effects on the CP-AMPAR-mediated current without affecting the CIP-AMPAR-mediated current.

Due to the fast desensitization feature of AMPA receptors, the underestimation of the peak value of AMPA-current elicited by glutamate is almost unavoidable even using the fast drug-application system. Therefore, KA, a full agonist of AMPARs, was also used in our experiment to elicit the maximal AMPA-current without desensitization. The results obtained from these two sets of parallel experiments were basically compatible, in a sense that application of 10 μM Zn^{2+} significantly potentiated the CP-AMPAR-responses elicited by both glutamate and KA, either through eliminating the desensitization or enhance the response amplitude; meanwhile, the inhibition by 1 mM Zn^{2+} were both exhibited in glutamate- and KA-elicited CP-AMPAR-responses, with the only difference being the amplitude of down-regulation.

It has been reported that NMDARs are also expressed on the carp retinal H1 cells (Shen et al., 2006; Jiang et al., 2008; Wang et al., 2008). However, the activation of NMDA-current needs the co-application of glycine and glutamate in the absence of Mg^{2+}, when the membrane potential is clamped at –60 mV. Furthermore, previous reports have demonstrated that carp retinal HCs do not express kainate-type glutamate receptors (Lu et al., 1998; Okada et al., 1999; Schultz et al., 2001). Therefore the glutamate-responses recorded in our experiments, no matter elicited by glutamate or KA, was merely mediated by AMPARs and the complete inhibition of the glutamate-current by the co-application of NAS and PB confirmed this point.

The immunocytochemical localization studies suggest that carp retinal HCs are only labeled with GluR2/3 subunits of glutamate receptors (Schultz et al., 2001), which implies that the HCs might express CIP-AMPARs. On the other hand, studies using Ca^{2+} imaging technique revealed that the AMPARs expressed on these cells actually had a high Ca^{2+} permeability (Okada et al., 1999; Huang et al., 2004; Huang and Liang, 2005). Based on the immunocytochemical studies and functional analysis of intracellular Ca^{2+} signal, it leads to the inference that CP- and CIP-AMPARs should be co-expressed on the HCs, whereas our experiments directly examined the membrane-current contribution of these two AMPAR subtypes and indicate that in the retinal H1 cells, the CP-AMPARs contribute a larger fraction to the glutamatergic synaptic response as compare to the co-existed CIP-AMPARs. To analyze the CP-AMPAR-mediated current in H1 cells, NAS, the specific CP-AMPAR blocker was applied. The partial recovery (about 65.0% of the control levels) after NAS-application (Fig. 2) was resulted from the toxic effect of NAS which was difficult to be washed out completely (see also Koike et al., 1997).

The large proportion of glutamate-current mediated by CP-AMPARs on HCs might be related to the cell's physiological and pathological functions. In the outer plexiform layer of retina, HCs are directly postsynaptic to photoreceptors, receiving glutamatergic input from photoreceptors, and releasing GABA in the dark, the latter might be involved in the inhibitory feedback from HCs to photoreceptors, although the mechanism for this feedback pathway is still controversial (Kaneko and Tachibana, 1986; Hirasawa and Kaneko, 2003; Tatsukawa et al., 2005; Cadetti and Thoreson, 2006). The CP-AMPARs may play important roles in those physiological processes to regulate the synaptic connectivity between photoreceptors and HCs. On one hand, the feedforward pathway between photoreceptor and post-synaptic horizontal cell was modifiable and the modifiability was eliminated when the CP-AMPARs on HCs were blocked (Huang et al., 2006); on the other hand, Ca^{2+} entering through the CP-AMPARs also inhibits GABA transport-current in HCs (Kreitzer et al., 2003), which affects the GABA concentration in the synaptic cleft and thus might regulate the GABAergic signals back to photoreceptors, which was hypothesized to be involved in creating the surround portion of the classic center-surround receptive fields of retinal neurons (Tachibana and Kaneko, 1984;

Kaneko and Tachibana, 1986; Tatsukawa et al., 2005). In addition to the physiological functions in synaptic plasticity, CP-AMPARs are also involved in the pathological excitotoxicity under retinal ischemia (for reviews, see Ugarte and Osborne, 2001; Kwak and Weiss, 2006).

In the retina, Zn^{2+} has been reported to exhibit a monotonic dose-dependent suppression of the glutamate-response in bass retinal HCs, which is mediated by AMPA receptors (Zhang et al., 2002). In our present study, the results demonstrate the dual effects of Zn^{2+} in isolated retinal HCs: potentiating the CP-AMPAR mediated response at a low concentration (10 μM Zn^{2+}), while inhibiting the response at higher concentration (100 μM and 1 mM Zn^{2+}). Such dual effects were also previously observed on the AMPARs in cultured superior colliculus neurons (Bresink et al., 1996). Our results seem to suggest that at low concentration, Zn^{2+} potentiates the CP-AMPAR-response on HCs and this potentiation might be related to the physiological activities of CP-AMPARs on HCs; whereas during excitotoxicity, Zn^{2+}, which is accumulated in the synaptic cleft and then reaches a high concentration, begins to inhibit the activity of CP-AMPARs, preventing the neurons from further Ca^{2+}/Zn^{2+} influx through these receptors and then slows down the cell death.

Although the mechanism(s) underlying the dual-effect that Zn^{2+} exerts on CP-AMPARs is/are not yet well understood, the different effects are likely mediated by separate mechanisms. The Zn^{2+}-binding site is most likely to be located on the external side of AMPARs, since these receptors subunits (GluR1–4) possess a large N-terminal domain (NTDs), which may harbor Zn^{2+} binding sites, like NMDA receptors (Gielen et al., 2008; Paoletti et al., 2009). Such structural property is compatible with the results reported by Zhang et al., 2002 that Zn^{2+} inhibitory effect on AMPARs was observed from both whole cell and excised outside-out patch recordings (with Zn^{2+} concentrations of 3–300 μM), which suggests that the Zn^{2+} inhibitory effect is mediated by the mechanism related to external biding-site (Zhang et al., 2002). In our present study, Zn^{2+} at higher concentrations (≥100 μM) showed similar inhibitory effect on CP-AMPARs (see Fig. 4Ab, Ac, Bb, Bc), which might also result from the external binding of Zn^{2+} on these receptors. However, at lower concentration (10 μM), it was observed in our experiment that Zn^{2+} potentiate CP-AMPAR-mediated response (see Fig. 4Aa, Ba) and attenuate the CP-AMPAR desensitizing (see Fig. 4Aa), which is similar to the cyclothiazide (CTZ) effect on AMPARs and is thus probably resulted from the interaction with CTZ-binding site on these receptors. If these explanations stand, the different Zn^{2+}-binding sites mediating potentiation and inhibition effects may be with a high and low Zn^{2+} affinity respectively. In addition, the dual effects that Zn^{2+} exerted on CP-AMPARs did not change the receptor's affinity for glutamate on carp retinal H1 HCs (see Fig. 6 and Table 2). It suggests that the Zn^{2+}-binding on CP-AMPARs to exert the dual effects does not compete with the glutamate-binding process; in other words, the Zn^{2+} effects do not exert at the agonist-recognition site of these receptors.

Overall, CP-AMPARs contribute the majority to the glutamatergic response and Zn^{2+} modulatory effect is involved in the CP-AMPARs mediated synaptic signaling pathways and might also play a neuroprotective role under excitotoxicity in carp retinal H1 cells.

4. Experimental procedures

4.1. *Preparation*

The experiments were performed on H1 horizontal cells isolated from adult carp (*Carassius auratus*, 15–20 cm body length) retinas, following the method previously described (Jiang et al., 2008), which strictly conformed to the humane treatment and use of animals as prescribed by the Association for Research in Vision and Ophthalmology. In brief, retina isolated from an eyeball was cut into 8–12 pieces, the retinal pieces were incubated in 4 ml Hank's solution with 25 U/ml papain and 4 mg L-cysteine for 30 min at 25 °C. The retinal pieces were rinsed and stored in the Hank's solution at 4 °C. Cells were freshly dissociated from the retinal pieces by gentle mechanical trituration in Ringer's solution and then the cell suspension was placed onto a plastic dish. H1 horizontal cell was easily distinguished by its characteristic morphology (Jiang et al., 2008).

4.2. *Solutions*

Hank's solution contained (in mM) 120.0 NaCl, 3.0 KCl, 0.5 $CaCl_2$, 1.0 $MgSO_4$, 1.0 Na-pyruvate, 1.0 NaH_2PO_4, 0.5 $NaHCO_3$, 20.0 HEPES and 16.0 glucose. Normal Ringer's solution contained (in mM) 120.0 NaCl, 5.0 KCl, 2.0 $CaCl_2$, 1.0, $MgCl_2$, 10.0 HEPES and 16.0 glucose. The pH value of these two solutions was adjusted to 7.4 with NaOH. Glutamate (Glu), kainate (KA), 1-naphthyl acetyl spermine (NAS), pentobarbital (PB) and $ZnCl_2$ (Zn^{2+}) were dissolved in the Ringer's solution. Glu and PB were freshly prepared just before the experiment. KA and NAS were prepared in high concentration of 20 mM and stored at –20 °C and then diluted to the required final concentration in the Ringer's solution before use. The intracellular solution for patch electrode contained (in mM) 140.0 CsCl, 0.05 $CaCl_2$, 1.0 $MgSO_4$, 0.5 EGTA, 10.0 HEPES. The pH value was adjusted to 7.3 with CsOH. All the drugs were purchased from Sigma (St Louis, MO, USA).

4.3. *Whole-cell recording and drug application*

Cells were voltage-clamped at –60 mV and whole-cell recordings were achieved by 5–8 MΩ patch pipette pulled from borosilicate glass (Sutter Instrument Inc., USA) using a horizontal puller (P87, Sutter Instrument Inc.). The pipette was filled with intracellular solution, mounted on a motor-driven micromanipulator (MC1000e, SD Instrument Inc.), and was connected to a patch amplifier (Axopatch 200B, Axon Instrument Inc., USA). An Ag/AgCl wire was used as a reference electrode. The liquid junction potential was compensated online. Fast capacitance, cell capacitance transients, and 70% of the series resistance of the recording electrode were compensated. Data acquisition was performed using AxoScope software (Axon Instrument Inc.), with sample rate being 1 kHz and was lowpass filtered (0–1 kHz). The recorded data were analyzed by Clampfit 9.2 software (Axon Instrument Inc.). All the drugs were applied using the superfusion system (DAD-12, ALA Scientific Instruments, USA). The statistical data are all presented in

the form of mean±SD in the text and mean±SE in the figure illustrations. Paired *t*-test was performed for statistical analysis otherwise stated.

Acknowledgments

This work was supported by grants from the State Key Basic Research and Development Plan (No. 2005CB724301), National Foundation of Natural Science of China (No. 30870836), the Ministry of Education (No. 20040248062) and Instrumental Analysis Center of SJTU.

REFERENCES

Bresink, I., Ebert, B., Parsons, C.G., Mutschler, E., 1996. Zinc changes AMPA receptor properties: results of binding studies and patch clamp recordings. Neuropharmacology 35, 503–509.

Cadetti, L., Thoreson, W.B., 2006. Feedback effects of horizontal cell membrane potential on cone calcium currents studied with simultaneous recordings. J. Neurophysiol. 95, 1992–1995.

Dingledine, R., Borges, K., Bowie, D., Traynelis, S.F., 1999. The glutamate receptor ion channels. Pharmacol. Rev. 51, 7–61.

Geiger, J.R., Melcher, T., Koh, D.S., Sakmann, B., Seeburg, P.H., Jonas, P., Monyer, H., 1995. Relative abundance of subunit mRNAs determines gating and Ca^{2+} permeability of AMPA receptors in principal neurons and interneurons in rat CNS. Neuron 15, 193–204.

Gielen, M., Le Goff, A., Stroebel, D., Johnson, J.W., Neyton, J., Paoletti, P., 2008. Structural rearrangements of NR1/NR2A NMDA receptors during allosteric inhibition. Neuron 57, 80–93.

Grahn, B.H., Paterson, P.G., Gottschall-Pass, K.T., Zhang, Z., 2001. Zinc and the eye. J. Am. Coll. Nutr. 20, 106–118.

Hirasawa, H., Kaneko, A., 2003. pH changes in the invaginating synaptic cleft mediate feedback from horizontal cells to cone photoreceptors by modulating Ca^{2+} channels. J. Gen. Physiol. 122, 657–671.

Hollmann, M., Heinemann, S., 1994. Cloned glutamate receptors. Annu. Rev. Neurosci. 17, 31–108.

Huang, S.Y., Liang, P.J., 2005. Ca^{2+}-permeable and Ca^{2+}-impermeable AMPA receptors coexist on horizontal cells. Neuroreport 16, 263–266.

Huang, S.Y., Liu, Y., Liang, P.J., 2004. Role of Ca^{2+} store in AMPA-triggered Ca^{2+} dynamics in retinal horizontal cells. Neuroreport 15, 2311–2315.

Huang, S.Y., Hu, J.F., Gong, H.Q., Liang, P.J., 2006. Postsynaptic calcium pathway contributes to synaptic plasticity between retinal cones and luminosity-type horizontal cells. Sheng Li Xue Bao 58, 407–414.

Jiang, X.D., Wang, X.L., Sun, Y., Gong, H.Q., Liang, P.J., 2008. NMDA modulation of GABA transporter current in carp retinal horizontal cells. Brain Res. 1240, 105–110.

Kaneko, A., Tachibana, M., 1986. Effects of gamma-aminobutyric acid on isolated cone photoreceptors of the turtle retina. J. Physiol. 373, 443–461.

Koike, M., Iino, M., Ozawa, S., 1997. Blocking effect of 1-naphthyl acetyl spermine on Ca^{2+}-permeable AMPA receptors in cultured rat hippocampal neurons. Neurosci. Res. 29, 27–36.

Kreitzer, M.A., Andersen, K.A., Malchow, R.P., 2003. Glutamate modulation of GABA transport in retinal horizontal cells of the skate. J. Physiol. 546, 717–731.

Kwak, S., Weiss, J.H., 2006. Calcium-permeable AMPA channels in neurodegenerative disease and ischemia. Curr. Opin. Neurobiol. 16, 281–287.

Lee, S.C., Zhong, Y.M., Li, R.X., Yu, Z., Yang, X.L., 2008. Localization of zinc in the outer retina of carp: a light- and electron-microscopic study. Synapse 62, 352–357.

Lu, T., Shen, Y., Yang, X.L., 1998. Desensitization of AMPA receptors on horizontal cells isolated from crucian carp retina. Neurosci. Res. 31, 123–135.

Okada, T., Schultz, K., Geurtz, W., Hatt, H., Weiler, R., 1999. AMPA-preferring receptors with high Ca^{2+} permeability mediate dendritic plasticity of retinal horizontal cells. Eur. J. Neurosci. 11, 1085–1095.

Paoletti, P., Vergnano, A.M., Barbour, B., Casado, M., 2009. Zinc at glutamatergic synapses. Neuroscience 158, 126–136.

Partin, K.M., Bowie, D., Mayer, M.L., 1995. Structural determinants of allosteric regulation in alternatively spliced AMPA receptors. Neuron 14, 833–843.

Redenti, S., Ripps, H., Chappell, R.L., 2007. Zinc release at the synaptic terminals of rod photoreceptors. Exp. Eye Res. 85, 580–584.

Schmidt, K.F., 1999. Divalent cations modulate glutamate receptors in retinal horizontal cells of the perch (*Perca fluviatilis*). Neurosci. Lett. 262, 109–112.

Schultz, K., Janssen-Bienhold, U., Weiler, R., 2001. Selective synaptic distribution of AMPA and kainate receptor subunits in the outer plexiform layer of the carp retina. J. Comp. Neurol. 435, 433–449.

Shen, Y., Yang, X.L., 1999. Zinc modulation of AMPA receptors may be relevant to splice variants in carp retina. Neurosci. Lett. 259, 177–180.

Shen, Y., Zhang, M., Jin, Y., Yang, X.L., 2006. Functional N-methyl-D-aspartate receptors are expressed in cone-driven horizontal cells in carp retina. Neurosignals 15, 174–179.

Sommer, B., Keinanen, K., Verdoorn, T.A., Wisden, W., Burnashev, N., Herb, A., Kohler, M., Takagi, T., Sakmann, B., Seeburg, P.H., 1990. Flip and flop: a cell-specific functional switch in glutamate-operated channels of the CNS. Science 249, 1580–1585.

Tachibana, M., Kaneko, A., 1984. γ-Aminobutyric acid acts at axon terminals of turtle photoreceptors: difference in sensitivity among cell types. Proc. Natl. Acad. Sci. U. S. A. 81, 7961–7964.

Tatsukawa, T., Hirasawa, H., Kaneko, A., Kaneda, M., 2005. GABA-mediated component in the feedback response of turtle retinal cones. Vis. Neurosci. 22, 317–324.

Taverna, F.A., Cameron, B.R., Hampson, D.L., Wang, L.Y., MacDonald, J.F., 1994. Sensitivity of AMPA receptors to pentobarbital. Eur. J. Pharmacol. 267, R3–5.

Ugarte, M., Osborne, N.N., 2001. Zinc in the retina. Prog. Neurobiol. 64, 219–249.

Van Damme, P., Van Den Bosch, L., Van Houtte, E., Callewaert, G., Robberecht, W., 2002. GluR2-dependent properties of AMPA receptors determine the selective vulnerability of motor neurons to excitotoxicity. J. Neurophysiol. 88, 1279–1287.

Wang, X.L., Jiang, X.D., Liang, P.J., 2008. Intracellular calcium concentration changes initiated by N-methyl-D-aspartic acid receptors in retinal horizontal cells. Neuroreport 19, 675–678.

Wu, S.M., Qiao, X., Noebels, J.L., Yang, X.L., 1993. Localization and modulatory actions of zinc in vertebrate retina. Vis. Res. 33, 2611–2616.

Yamakura, T., Sakimura, K., Mishina, M., Shimoji, K., 1995. The sensitivity of AMPA-selective glutamate receptor channels to pentobarbital is determined by a single amino acid residue of the alpha 2 subunit. FEBS Lett. 374, 412–414.

Zhang, D.Q., Ribelayga, C., Mangel, S.C., McMahon, D.G., 2002. Suppression by zinc of AMPA receptor-mediated synaptic transmission in the retina. J. Neurophysiol. 88, 1245–1251.